DALTON
FULL PAPER

Preparation of [VO(sal-L-Trp)(H_2O)] (sal-L-Trp = *N*-salicylidene-L-tryptophanate) and characterisation of an unusual product obtained from its solutions in water–pyridine

João Costa Pessoa,*[a] Maria Teresa Duarte,[a] Robert D. Gillard,*[b] Catarina Madeira,[a] Pedro M. Matias[c] and Isabel Tomaz[a]

[a] *Centro Química Estrutural, Instituto Superior Técnico, Av. Rovisco Pais, 1049-001 Lisboa, Portugal. E-mail: pcjpessoa@alfa.ist.utl.pt*
[b] *Department of Chemistry, University of Wales, PO Box 912, Cardiff, UK CF1 3TB*
[c] *Instituto de Tecnologia Química e Biológica, Rua da Quinta Grande, 6, 2780 Oeiras, Portugal*

Received 23rd July 1998, Accepted 9th October 1998

A vanadium(IV) complex [VO(sal-L-Trp)(H_2O)] **1** (sal-L-Trp = *N*-salicylidene-L-tryptophanate) has been isolated from solutions containing oxovanadium(IV), L-tryptophan and salicylaldehyde. From solutions also containing quinolin-8-ol (Hhquin) a similar oxovanadium(IV) complex VO(sal-L-Trp)·Hhquin·$2H_2O$ **2** was isolated. From solutions of **1** in water–pyridine, orange-brown crystals of $[Hpy^+]_4[C_{14}H_{13}N_2^+]_2[V_{10}O_{28}^{6-}]$ **3** were isolated and characterised by X-ray diffraction. The mechanism proposed for this reaction involves the attack of a pyridine molecule at the β-carbon atom of the tryptophan residue in **1**.

Introduction

Studies[1–10] concerning the preparation and reactivity of complexes of vanadium with *N*-salicylideneamino acids have been made and some unusual organic reactions have been reported recently involving such systems.[9,11] The present study describes the preparation and characterisation of $[V^{IV}O(sal\text{-}L\text{-}Trp)(H_2O)]$ **1** (sal-L-Trp = *N*-salicylidene-L-tryptophanate) and the preparation of a similar complex **2** containing protonated neutral quinolin-8-ol (Hhquin) is outlined. From solutions of **1** in water–pyridine, brown crystals of $[Hpy^+]_4[L^+]_2[V_{10}O_{28}^{6-}]$ **3** (py = pyridine; $L^+ = C_{14}H_{13}N_2^+$, a product of condensation of the tryptophan side group with pyridine) have been isolated after 3–4 weeks and characterised by X-ray crystallography. A plausible mechanism for the formation of L^+ is discussed.

Results and discussion

Fig. 1 shows the visible circular dichroism spectrum of complex **1** (curve B). Five bands are clear for $\lambda > 420$ nm: four probably correspond to d–d transitions, emphasising the non-symmetrical nature of the ligand field; at least one of the bands around 450 nm is a LMCT band. This spectrum resembles those for several other complexes[5] of the type [VO(sal-L-aa)(H_2O)] (sal-L-aa = *N*-salicylidene-L-amino carboxylate with non-co-ordinating side chains) although the bands at $\lambda \approx 455$ nm (one of them possibly band III: $d_{xy} \longrightarrow d_{z^2}$) are better defined in the present case. When the solution contains bipy the pattern of the spectrum remains the same but band Ia shifts to the UV by *ca.* 50 nm, and bands Ib, II both shift to the red by *ca.* 12 nm. Again this behaviour is very similar to what was found[5] for other [VO(sal-L-aa)(H_2O)] complexes. Spectrum B (Fig. 1) changes with time. After ≈45 min the $|\Delta\varepsilon|$ for $\lambda >$ 600 nm decrease slightly but those for $\lambda < 600$ nm increase significantly. After ≈20 h only one intense band with $\lambda_{max} \approx 450$ nm may be seen in the CD spectrum in the range 420–1000 nm, consistent with the formation of a vanadium(V) complex. The absorption spectrum of **1** shows maxima (and absorption coefficients) at 275 (15400), 375 (4850), 520 (45) and 730 nm (20 $dm^3\ mol^{-1}\ cm^{-1}$), and all ε values increase with time. The main process occurring is the progressive oxidation of V^{IV} to V^V, the increase in $\Delta\varepsilon$ and ε values for $\lambda < 600$ nm being due to a charge transfer transition from phenolate oxygens to d orbitals of the Schiff base vanadium(V) complex formed.[12]

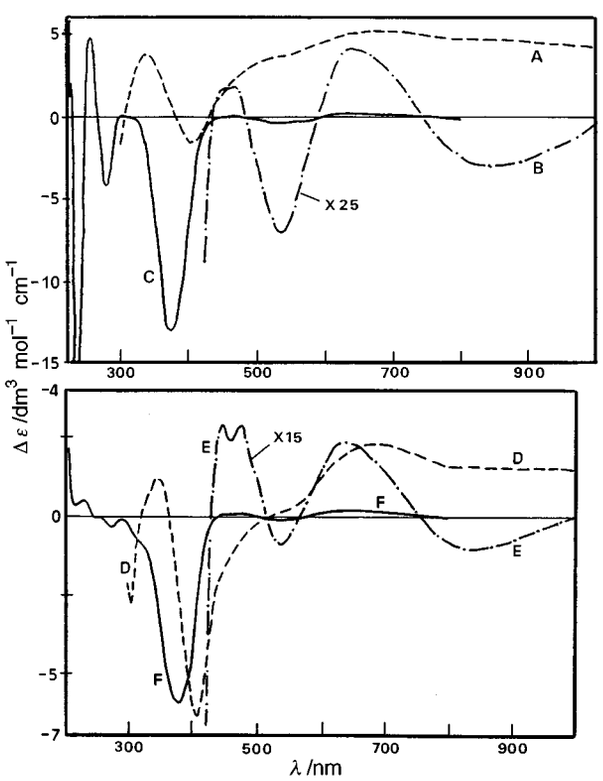

Fig. 1 Circular dichroism spectra of complexes **1** and **2** and of their solutions in methanol: **A** (------) **1** (solid dispersed in KBr disc), **B** (–·–·–) **1** in methanol (10^{-2} M solution), **C** (———) **1** in methanol (1.8×10^{-4} M solution), **D** (------) **2** (solid dispersed in KBr disc), **E** (–·–·–) **2** in methanol (3.6×10^{-4} M solution) and **F** (———) **2** in methanol (6.9×10^{-4} M solution).

The CD spectrum of complex **2** as a KBr disc (D in Fig. 1) is remarkably similar to that for **1** (spectrum A), so the main stereochemical features are the same in both: in particular, the co-ordination geometries must be similar. In the CD of **2** in

Table 1 Spin Hamiltonian parameters for complexes **1** and **2** in methanol (concentration ≈ 2×10^{-3} M)

Complex		$10^4 A_{\parallel}$/cm^{-1}	$g_{\parallel}$	$10^4 A_{\perp}$/cm^{-1}	$g_{\perp}$
1 [VO(sal-L-Trp)(H_2O)][a]		170.8	1.948	61.7	1.982
2a [VO(sal-L-Trp)-(Hhquin)][b]	(*ca.* 70%)	170.7	1.949	61.0	1.982
2b	(*ca.* 30%)	165.1	1.945	61.8	1.984

[a] Spin Hamiltonian parameters obtained by simulation of spectra using the program EPRPOW.[15] [b] The spin Hamiltonian parameters were calculated following the method described in ref. 13 by an iterative calculation procedure using the corrected equations given in ref. 16. Coincident perpendicular lines had to be assumed for **2a** and **2b** as a first approximation because these lines were not resolved.

methanolic solution the pattern of the bands is quite similar to that of **1** and the band assignments are the same. The spectrum depends on concentration and varies with time like that of **1**. The absorption spectrum of **2** is quite intense for $\lambda < 300$ and maxima (and ε values) are at 330 (≈6000), 375 (6300) and 485 nm (2000 dm^3 mol^{-1} cm^{-1}). Bands for $\lambda > 600$ nm are hidden under the tail of the LMCT band at 485 nm. As with **1**, oxidation of V^{IV} to V^{V} accounts for most of the changes observed with time.

In the UV range the oxovanadium(IV) complexes derived from salicylaldehyde generally possess a low-energy band around 375 nm which can be attributed to a $\pi \longrightarrow \pi^*$ transition originating mainly in the azomethine chromophore.[5] This occurs at 376 nm for **1** (shifting to 385 nm if the solution contains bipy) and at 378 nm for **2**. These bands display negative Cotton effects in CD, as found for other [VO(sal-L-aa)(X)] complexes (aa = Ala, Val, Phe, Met or Ile, X = H_2O, py or bipy).[3,5]

The ESR spectra may help elucidate which groups co-ordinate in equatorial position in solution. The spin Hamiltonian parameters for the species present in methanolic solutions of complexes **1** and **2** are in Table 1. These are as expected for complexes with the present donor atoms,[3,5,13,14] and with structures as found for other [VO(sal-L-aa)(X)] compounds. Component **2a** corresponds to a co-ordination geometry as for **1** in methanol, and the spin Hamiltonian parameters for **2b** (minor species) are in agreement with the presence of [V^{IV}O(sal-L-Trp)(hquin)]$^-$ with tridentate sal-L-Trp^{2-} equatorial and bidentate hquin$^-$ [O$^-$(phenolic) equatorial and N axial].

The magnetic susceptibilities of complexes **1** and **2** were measured in the range 5–290 K. For both complexes the μ_{eff} (see Experimental section) are within the values characteristic of monomeric oxovanadium(IV) complexes. We therefore suggest for **1** the structure schematically represented as **I**. For **2** the formulation differs from that of the *N*-salicylideneamino carboxylato complexes containing quinolin-8-olate previously known, which are all vanadium(V) compounds, *e.g.* [V^{V}O(sal-L-Gly)(hquin)],[8] [V^{V}O(sal-L-Phe)(hquin)][8] and [V^{V}O(L)(hquin)] where L = tridentate ONO Schiff base,[17] reduced Schiff base,[18] or ligands derived from aromatic *o*-hydroxyaldehydes or hydrazone compounds,[19] with O(phenolate) from hquin$^-$ co-ordinated equatorially. Thus **2** is clearly a vanadium(IV) complex, so quinolin-8-ol must be present as a neutral species (Hhquin) and if co-ordinated to vanadium this is either by N, by HO (phenolic) or both.

We know of only one case where Hhquin acts as a ligand. This is in the compound "[Pd(hquin)$_2$(HCN)$_2$]", reformulated[20] as *cis*-[Pd(CN)$_2$(Hhquin)$_2$], where the quinolin-8-ol ligands were attached to four-co-ordinated palladium(II) *via* their aromatic N donor units in a monodentate fashion. We consequently take both **1** and **2**, with their similar chiroptical properties, to be essentially five-co-ordinated at vanadium(IV). Clearly, the pendant phenolic group of monodentate Hhquin

Table 2 Selected bond distances (Å) and angles (°) for both cations $L^+ = C_{14}H_{13}N_2^+$

N31–C30	1.50(2)	N51–C50	1.61(2)
C36–C31	1.34(2)	C56–C51	1.23(2)
C32–N31	1.32(2)	C52–N51	1.324(14)
C30–C23	1.51(2)	C50–C43	1.48(2)
C23–C24	1.47(2)	C43–C44	1.36(2)
C23–C22	1.34(2)	C43–C42	1.34(2)
N31–C30–C23	114.2(11)	N31–C30–C23	113.9(11)
C22–C23–C24	108.6(11)	C42–C43–C44	104.4(13)
C22–C23–C30	124.2(13)	C42–C43–C50	120(2)
C24–C23–C30	127.0(11)	C44–C43–C50	135(2)
C32–N31–C36	120.6(14)	C52–N51–C56	113(2)
C36–N31–C30	119.6(14)	C56–N51–C50	123.0(14)
C32–N31–C30	119.6(12)	C52–N51–C50	123.6(13)

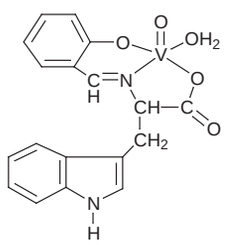

I

may form chelated structures *via* hydrogen bonding (or the phenolic OH may be also co-ordinated).

Brown crystals of [Hpy^+]$_4$[L^+]$_2$[$V_{10}O_{28}^{6-}$] **3** were isolated from aged (3–4 weeks) solutions of complex **1** in water–pyridine and characterised by X-ray diffraction. The crystal structure of **3** contains two independent decavanadate ions, each centred on a crystallographic inversion centre, and thus only half of each is independent. The asymmetric unit of this crystal structure further contains four pyridinium and two L^+ cations. A molecular diagram of one of the L^+ is shown in Fig. 2 with the atomic numbering scheme. Scheme 1 summarises the main process

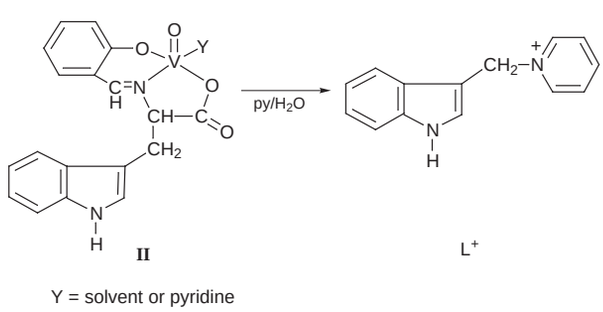

Scheme 1

emphasised here. Table 2 includes selected data from X-ray diffraction analysis for L^+. Bond distances and angles for the bridging -CH_2- (C30 and C50) both agree with sp^3 hybridisation for these carbons and the formation of single bonds connecting them to the N atom of the pyridine ring (C30–N31 and C50–N51) and to the indole ring (C30–C23 and C50–C43). Most other bond lengths and angles are as expected for pyridinium and indole groups.

A molecular diagram presenting the atomic numbering scheme for one of the decavanadate anions is shown in Fig. 3. The standard atomic numbering is used. The independent atoms are labelled A: the remainder, labelled B, are obtained from the corresponding A atoms by the symmetry operation $1 - x, -y, 2 - z$. This decavanadate can therefore be referred to as AB. A similar situation occurs for decavanadate CD (diagram not shown), the symmetry operation being $2 - x, -y, 1 - z$.

Table 3 Selected bond distances (Å) for $[V_{10}O_{28}]^{6-}$ in complex **3** and $(NH_4)_4Na_2V_{10}O_{28}\cdot 10H_2O$[4]

	decavanadate AB	decavanadate CD	Δ/σ	$(NH_4)_4Na_2V_{10}O_{28}\cdot 10H_2O$[4]
V1–O6	2.077(5)	2.112(5)	4.9	2.097(3)
V1–O6[a]	2.095(4)	2.096(5)	0.2	2.115(4)
V1–O7	1.960(5)	1.885(5)	10.6	1.920(4)
V1–O8[a]	1.948(5)	1.994(5)	6.5	1.916(3)
V1–O13	1.674(5)	1.680(5)	0.8	1.683(4)
V1–O15[a]	1.687(5)	1.675(5)	1.7	1.697(3)
V2–O2	1.597(6)	1.608(6)	1.4	1.618(4)
V2–O6	2.275(5)	2.255(5)	7.1	2.244(4)
V2–O7	2.052(5)	1.991(5)	8.6	2.000(4)
V2–O8	1.999(5)	2.040(5)	5.7	1.989(4)
V2–O23	1.843(5)	1.789(5)	7.6	1.820(4)
V2–O25	1.770(5)	1.827(5)	8.1	1.819(3)
V3–O3	1.601(5)	1.599(5)	0.3	1.602(4)
V3–O6	2.316(4)	2.331(5)	2.1	2.290(4)
V3–O13	2.051(5)	2.049(5)	0.3	2.056(3)
V3–O23	1.907(6)	1.902(5)	0.7	1.867(4)
V3–O34	1.846(5)	1.826(5)	2.8	1.886(4)
V3–O35	1.834(5)	1.836(5)	0.3	1.825(4)
V4–O4	1.599(5)	1.611(6)	1.5	1.619(4)
V4–O6	2.275(5)	2.250(5)	3.5	2.225(3)
V4–O7[a]	2.016(5)	1.977(5)	5.5	1.995(3)
V4–O8[a]	2.031(5)	2.066(5)	4.9	2.021(3)
V4–O34	1.813(5)	1.858(5)	6.4	1.809(4)
V4–O45	1.793(5)	1.758(6)	4.5	1.816(4)
V5–O5	1.606(5)	1.596(6)	1.3	1.598(4)
V5–O6	2.338(5)	2.339(5)	0.1	2.358(3)
V5–O15	2.039(5)	2.072(5)	4.6	2.019(4)
V5–O25	1.884(5)	1.862(6)	2.8	1.874(3)
V5–O35	1.823(5)	1.795(6)	3.6	1.850(4)
V5–O45	1.876(5)	1.922(6)	5.9	1.891(4)

[a] Symmetry-related atom, by $-x+1, -y, -z+2$ (AB) or $-x+2, -y, -z+1$ (CD).

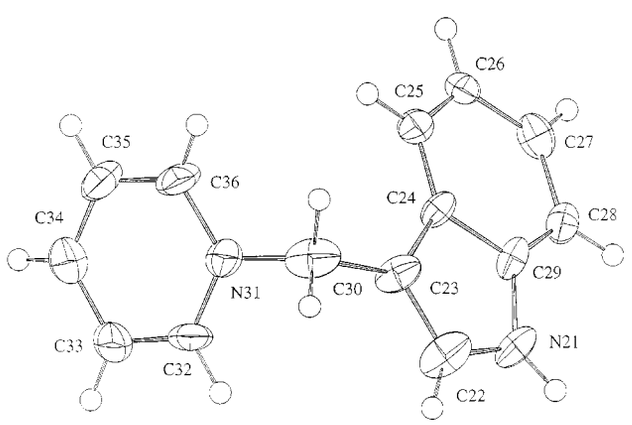

Fig. 2 An ORTEP[21] diagram of one of the $C_{14}H_{13}N_2^+$ ions showing the atomic notation. The notation used for the second ion of the same species (not shown) is similar, the 2 being added to first digit in each atom label. The thermal ellipsoids of the non-hydrogen atoms have been drawn at the 20% probability level, the hydrogen atoms with an arbitrary isotropic thermal parameter of 0.025 Å^2.

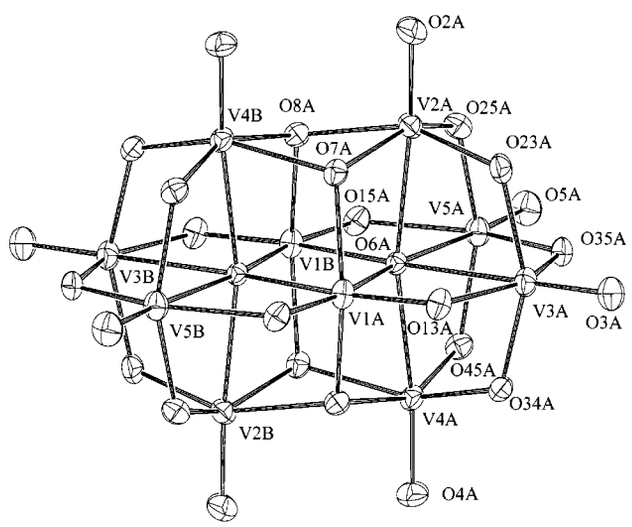

Fig. 3 An ORTEP[21] diagram of $[V_{10}O_{28}]^{6-}$ showing the atomic notation of molecule AB. The notation used for decavanadate CD (not shown) is similar. The thermal ellipsoids have been drawn at the 30% probability level. For clarity, only the vanadium atoms in part B are labelled.

Selected bond distances for both decavanadate ions in the asymmetric unit are listed side by side in Table 3 and the agreement is reasonable, although one third (ten out of thirty) of the differences between corresponding distances is greater than 5σ, with only one [V1–O7, 1.960(5) *vs.* 1.885(5) Å] being greater than 10σ. These differences may indeed result from different environments in the crystal structure. However in view of the quality of the available diffraction data (as measured from some of the indices in Table 5), the standard deviations of the atomic parameters may have been slightly underestimated, giving rise to an artificially high statistical significance for these differences.

There are six intermolecular hydrogen bonds between decavanadates AB and CD and the six other molecular ions in the asymmetric unit. These are listed in Table 4, where N21 and N41 are indole N atoms and N61, N71, N81 and N91 are N atoms from Hpy^+ cations. The hydrogen bonding patterns of the two independent decavanadate ions in the unit cell are quite different, one interacting with six pyridinium cations and the other with two pyridinium cations and four L^+ ions.

The decavanadate formed by oxidation of V^{IV} by atmospheric oxygen. Although the vanadium concentration in the preparation of complex **3** is relatively high (nearly saturated solution of **1**) the formation of a decavanadate from these alkaline solutions is surprising. However it is not uncommon that rather insoluble species form from solutions where they are present in minor concentrations. If the $[V_{10}O_{28}]^{6-}$ were protonated, some V–O bonds in **3** would differ significantly in length from those of its counterpart $Na_6V_{10}O_{28}\cdot 18H_2O$[22] which is

Table 4 Hydrogen bonds for $[Hpy^+]_4[C_{14}H_{13}N_2^+]_2[V_{10}O_{28}^{6-}]$ **3**

D···H group	O	Distance (H···O)/Å	Angle (N–H···O)/°
N21···H21 ($x, y-1, z$)	O4C	2.13(1)	162(1)
N41···H41 ($1-x, y-\frac{1}{2}, \frac{1}{2}-z$)	O23C	2.16(1)	151(1)
N61···H61 ($x, \frac{1}{2}-y, \frac{1}{2}+z$)	O8C	1.70(1)	174(1)
N71···H71 ($1-x, y-\frac{1}{2}, \frac{3}{2}-z$)	O7A	1.90(1)	166(1)
N81···H81 ($1-x, -y, 1-z$)	O8A	1.86(1)	165(1)
N91···H91 ($1-x, y-\frac{1}{2}, \frac{3}{2}-z$)	O23A	1.74(1)	171(1)

certainly unprotonated. Any such difference would help in locating any proton in **3**. However, the small differences found in the eight-membered V_4O_4 rings (*e.g.* V1–O8–V2–O23–V3–O34–V4–O7, V1–O7–V2–O25–V5–O45–V4–O8) indicate a $[V_{10}O_{28}]^{6-}$ formulation. The spacings between the different atom layers, estimated from the spacings between their respective least-squares planes,[4,23] are comparable with similar values from other $[V_{10}O_{28}]^{6-}$ decavanadates.[4,22] This too indicates that the decavanadates of **3** are not protonated.

IR spectra

Complex **1** exhibits a broad medium OH band at 3500–2800 cm^{-1} (maximum at 3065 cm^{-1}) with a sharp medium band emerging at 3480 cm^{-1} corresponding to ν(N–H). The spectrum of **2** is consistent with the formulation as a complex containing Hhquin. The sharp indole N–H peak of tryptophan at 3495 cm^{-1} agrees in energy with that of the congener in **1**, the aqua complex. However, the nature of the broad background in **2** is quite distinct from that in **1**. For **2**, the broad strong absorption at 3600–2800 cm^{-1} is maximal at *ca.* 3400 cm^{-1}, strongly suggesting a hydrogen bonded phenolic OH unit. Relatively broad and strong bands at 1630 and 1600 cm^{-1} (for **1**) and 1627 and 1602 cm^{-1} (for **2**) correspond to ν(C=N) and $\nu_{asym}(CO_2)$, respectively; these bands are broadened because of overlap with aromatic ring-carbon stretching. The two medium bands at 970 or 1002 cm^{-1} could be ascribed to ν(V=O); in the FTIR of **1** only one strong band at 1002 cm^{-1} can be ascribed to ν(V=O). The C–H out-of-plane deformations, characteristic of the 1,2-disubstituted benzene ring of tryptophan,[24] are at 756 cm^{-1} for **1** and 748 cm^{-1} for **2**. Overall the main features of the IR spectra of **1** and **2** are comparable with those reported for the two $[Cu(sal\text{-}Trp)(H_2O)_2]$ complexes characterised by X-ray analysis.[25]

For complex **3** the absorptions due to stretching of bonds to hydrogen appear as a broad hump centred at *ca.* 3300 cm^{-1}, with distinct, less broad absorptions emerging at *ca.* 3050 and 3350 cm^{-1}. These we assign respectively to the aromatic C–H of pyridinium and of indole in L^+, and to the NH of the new indole unit in L^+.

Mechanism proposed for the formation of L^+

The formation of complexes with structures such as **II** (Scheme 1 or 2) is well documented.[3–5,9,26] The formation of $L^+ = C_{14}H_{13}N_2^+$ as a product of the condensation of the tryptophan side group with pyridine (see below) was confirmed by the characterisation by X-ray single crystal diffraction of complex **3**. A possible pathway for this reaction involves the attack of a pyridine molecule at the β-carbon atom of the tryptophan residue in **II**, leading to the elimination of the side group of this amino acid; this produces **III** (Scheme 2) which may react with a proton (*e.g.* from a water molecule) to yield the complex containing *N*-salicylideneglycinate. In HPLC experiments with samples of the reaction mixture of one of the batches for the synthesis of **3** (after pre-column derivatisation with the *o*-phthalaldehyde–2-sulfanylethanol reagent solution) a band corresponding to glycine was detected. On spiking the reaction mixture with glycine only this band increases in intensity, confirming the identification of this amino acid.

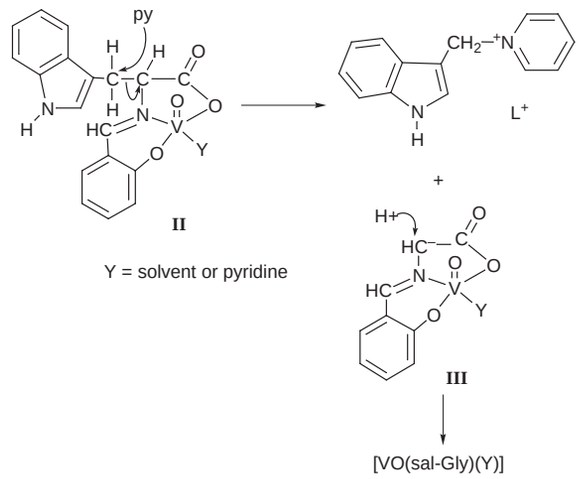

Scheme 2

Vanadium is one of the most active metal ions in β-eliminations.[1,2,27] These probably proceed by the mechanism proposed by Metzler *et al.*[28] for the pyridoxal-catalysed reactions, which involves the formation of a Schiff base complex (pyridoxal = 3-hydroxy-5-hydroxy-methyl-2-methylpyridine-4-carbaldehyde).

The present system presumably involves an oxovanadium(IV or V) Schiff base complex **II** (Scheme 2), where pyridine or water may be co-ordinated in equatorial and/or in axial position.[3,9] By an intramolecular or intermolecular pyridine attack on the β-carbon of the amino acid moiety, L^+ may form. Species **III** (Scheme 2) yields the Schiff base complex of glycine. Hydrolysis at the imine bond yields free glycine. Pyruvate and ammonia are final products of α,β-eliminations catalysed by several pyridoxal containing enzymes[29,30] and in model systems involving activation by vanadium.[31] Such further reactions do not proceed efficiently in our reaction mixtures as significant amounts of glycine and tryptophan remain in the mixture for several weeks.

The reversal of rather similar reactions activated by metal ions in complexes of *N*-salicylideneamino carboxylate systems has been described (*e.g.* refs. 32 and 33) but to our knowledge there is only one example in model systems of a reaction involving the entire substituent group of tryptophan:[34] this involves the production of tryptophan from [Cu(N-carbethoxyethyl)-salicylaldiminate)$_2$] and gramine.

Conclusion

The close similarity of the spectroscopic properties (EPR, CD, UV/VIS and IR) between $[VO(sal\text{-}L\text{-}Trp)(H_2O)]$ **1** and several $[VO(sal\text{-}L\text{-}aa)(H_2O)]$ compounds previously studied[3,5] indicates that the co-ordination geometry and the main factors that determine the pattern of the solution CD spectra are the same. The complex VO(sal-L-Trp)·Hhquin·$2H_2O$ **2** is the first oxovanadium(IV) compound obtained from reaction mixtures containing Schiff base and related ligands and quinolin-8-ol. Its co-ordination geometry in the solid state is probably identical to that of **1**; Hhquin if co-ordinated to vanadium is either by N, by OH (phenolic) or both. The remarkable new cleavage (Scheme 2) of tryptophan at its asymmetric carbon, like other unusual processes in [VO(sal-aa)(X)],[9,11] emphasises the rich and often unexpected reactivities of these systems.

Experimental

Preparations

[VO(sal-L-Trp)(H$_2$O)] 1. To 50 mL of an aqueous solution of

L-tryptophan (2.8 mmol) containing sodium acetate (5.4 mmol) at 50 °C, salicylaldehyde (2.8 mmol) in ethanol (7 mL) was added. Vanadyl sulfate pentahydrate (2.4 mmol) in 2 mL of water was slowly added. A green solid formed, which was collected, washed with water and ethanol–water (50 : 50) and dried. Yield ≈ 30% (Found: C, 55.2; H, 4.2; N, 7.1. $C_{18}H_{16}N_2O_5V$ requires C, 55.25; H, 4.12; N, 7.16%). Mass spectroscopy (FAB) peaks at *m/z* 390/392, 374, 131, and others, consistent with the presence of [VO(sal-L-Trp)(H_2O)] **1**.

VO(sal-L-Trp)·Hhquin·2H_2O 2. To 80 mL of an aqueous solution of L-tryptophan (4.6 mmol) containing sodium acetate (9.1 mmol) at 50 °C, salicylaldehyde (4.6 mmol) and quinolin-8-ol (4.0 mmol) in ethanol (16 mL) were added, the solution becoming dark orange. Vanadyl sulfate pentahydrate (4.1 mmol) in 6 mL of water was slowly added. A dark green compound formed immediately which was collected, washed as described for **1**, and dried. Yield ≈ 57% (Found: C, 58.2; H, 4.1; N, 7.5; Na^+, ≈0. $C_{25}H_{24}N_3O_7V$ requires C, 58.60; H, 4.37; N, 7.59%).

[Hpy$^+$]$_4$[L$^+$]$_2$[$V_{10}O_{28}^{6-}$] 3. From solutions of complex **1** in water–pyridine, orange-brown crystals of **3** (L^+ as in Scheme 1) were isolated after 3–4 weeks and characterised by X-ray diffraction, elemental analysis (Found: C, 34.0; H, 2.9; N, 6.6. $C_{48}H_{52}N_8O_{28}V_{10}$ requires C, 33.95; H, 3.09; N, 6.60%), and IR. Several batches were made, **3** always being obtained. Yield ≈ 20%.

Apparatus

X-Ray measurements were made with an Enraf-Nonius CAD-4 diffractometer and graphite monochromatised Mo-Kα radiation (λ 0.71069 Å). The CD spectra were run on a JASCO 720 spectropolarimeter either at 200–700 nm or with a red-sensitive photomultiplier, UV/VIS with a Perkin-Elmer Lambda 9 spectrophotometer, ESR spectra on a Bruker 200d (connected to a Bruker B-MN C5) spectrometer, and IR with a Unicam Mattson FTIR spectrometer. For solution CD spectra, oxygen was removed from the solvents by bubbling N_2. The cells had their stoppers reinforced with Parafilm strips but no special care was taken to remove oxygen. The CD of complexes dispersed in KBr discs were recorded as described previously.[3,5]

Magnetic susceptibilities

The magnetic susceptibilities of complexes **1** (38.95 mg) and **2** (53.46 mg) were measured by the Faraday method with a MANICS Magnetometer-Susceptometer in the range 5–290 K. The results can be fitted by $\chi = C/(T - \theta)$, the Curie–Weiss law, particularly for $T > 100$ K for best evaluation of θ.[35] For **1**, $\chi_d = -1.9 \times 10^{-4}$ emu mol^{-1}, $\theta = 10.4$ K and $C = 0.318$ emu K mol^{-1}. At 290 K $\mu_{eff} = 1.76$ μ_B per V atom and the magnetic moments are approximately constant till 60 K ($\mu_{eff} = 1.72$ μ_B) and increase slightly as T continues to decrease till 5 K: $\mu_{eff} = 1.87$ μ_B. For **2**, $\chi_d = -2.8 \times 10^{-4}$ emu mol^{-1}, $\theta = -21.5$ K and $C = 0.417$ emu K mol^{-1}. At 290 K $\mu_{eff} = 1.76$ μ_B per V atom and again the magnetic moments are approximately constant decreasing very slightly till 70 K ($\mu_{eff} = 1.67$ μ_B), then increasing slightly as T continues to decrease till 6 K: $\mu_{eff} = 1.77$ μ_B.

HPLC

Apparatus. The HPLC system consisted of a JASCO 880-PU pump, a Rheodyne 7125 sampling valve with a 20 μL sample loop, a Merck LichroCART® guard column, a LichroCART® 250 × 4 Lichrosphere® C_{18} column and a JASCO 821-FP fluorescence detector.

Reagents and mobile phases. Unless otherwise stated, all products were Merck p.a. reagent grade. Methanol, water and THF were Lichrosolv® products. 2-Sulfanylethanol, *o*-phthalaldehyde (for fluorometry) and boric acid were used as received. The eluent used for amino acid analysis contained 30% methanol, 10% THF and 60% acetate buffer (0.1 M, pH 6.8), and the flow rate was 1.2 mL min^{-1}.

Procedure. For amino acid analysis the well established method involving pre-column derivatisation with an *o*-phthalaldehyde–2-sulfanylethanol reagent solution and fluorescence detection ($\lambda_{ex} = 335$ and $\lambda_{em} = 450$ nm) was used (*e.g.* refs. 36–38). Procedures for the reagent solution and the derivatization to the isoindole derivatives were according to Evens *et al.*[37]

Table 5 Final refinement statistics for [$C_5H_5NH^+$]$_4$[$C_{14}H_{13}N_2^+$]$_2$[$V_{10}O_{28}^{6-}$] **3**

Refinement method	Full-matrix least-squares on F^2
Calculated weights	$w = 1/[\sigma^2(F_o^2) + (0.0588P)^2 + 43.00P]$ where $P = [\max(F_o^2,0) + 2F_c^2]/3$
No. refined parameters	853
No. restraints	5
No. used reflections ($F_o > 0$)	10268
$R1$ (F)	0.1025
wR (F^2)	0.1771
Goodness of fit S	1.054
$\Delta\rho_{max}$, $\Delta\rho_{min}$/e Å^{-3}	1.6(1), −0.9(1)

Crystallography

Crystal data. [$C_5H_5NH^+$]$_4$[$C_{14}H_{13}N_2^+$]$_2$[$V_{10}O_{28}^{6-}$], $M_r = 1696.4$, monoclinic, space group $P2_1/c$, $a = 15.581(1)$, $b = 22.880(2)$, $c = 16.718(1)$ Å, $\beta = 91.696(5)°$, $V = 5957.2(7)$ Å^3, $Z = 4$, $F(000) = 3392$, $D_c = 1.891$ Mg m^{-3}, μ(Mo-Kα) = 1.588 mm^{-1}. 12114 Reflections measured, 11675 unique ($R_{int} = 0.0513$, $R_{\sigma(I)} = 0.0629$), 10268 with positive F_o, which were used in all calculations.

Structure determination and refinement. The positions of the ten vanadium atoms were determined by a direct method with the program SHELXS 86.[39] The remaining non-hydrogen atoms in each of the eight molecular moieties in the asymmetric unit were found from subsequent refinements followed by Fourier-difference syntheses. Following convergence of the anisotropic refinement, no hydrogen atoms could be located from the difference electron density map: therefore, all were placed in calculated positions and included in the refinement using the riding model. Group isotropic thermal motion parameters were refined for the hydrogen atoms, one for each of the eight molecular moieties in the asymmetric unit. Owing to geometry distortion caused by high thermal motion parameters in one of the L^+ cations, the bonds involving atoms C44 to C49 were restrained to be the same as those involving similar atoms C24 to C29, which had normal thermal motion parameters. The structure refinement calculations were carried out using program SHELXL 93.[40] The final refinement statistics are presented in Table 5. An unusually high residual peak of 1.6(1) e Å^{-3} was observed in the final difference electron density map. This peak was located near one of the pyridinium ions, suggesting positional disorder for this ion which could not be satisfactorily modelled.

CCDC reference number 186/1197.

Acknowledgements

We thank Fundação Calouste Gulbenkian, Fundo Europeu para o Desenvolvimento Regional, Fundação para a Ciência e Tecnologia, and project PRAXIS/2/2.1/QUI/151/94 for financial support, and Dr N. Clos, Servei de Magnetoquimica, Universitat de Barcelona for the magentic measurements.

References

1 F. Bergel, K. R. Harrap and A. M. Scott, *J. Chem. Soc.*, 1962, 1101.
2 Y. Murakami, H. Kondo and A. E. Martell, *J. Am. Chem. Soc.*, 1973, **95**, 7138.
3 I. Cavaco, J. Costa Pessoa, D. Costa, M. T. L. Duarte, P. M. Matias and R. D. Gillard, *J. Chem. Soc.*, *Dalton Trans.*, 1994, 149.
4 I. Cavaco, J. Costa Pessoa, S. Luz, M. T. L. Duarte, P. M. Matias, R. T. Henriques and R. D. Gillard, *Polyhedron*, 1995, **14**, 429.
5 I. Cavaco, J. Costa Pessoa, D. Costa, M. T. L. Duarte, R. T. Henriques, P. M. Matias and R. D. Gillard, *J. Chem. Soc.*, *Dalton Trans.*, 1996, 1989.
6 I. Cavaco, J. Costa Pessoa, D. Costa, M. T. L. Duarte, R. D. Gillard and P. M. Matias, *J. Inorg. Biochem.*, 1993, **51**, 157 and refs. therein.
7 S. Dutta, S. Mondal and A. Chakravorty, *Polyhedron*, 1995, **14**, 1163.
8 S. Dutta, S. Mondal and A. Chakravorty, *J. Chem. Soc.*, *Dalton Trans.*, 1995, 1115.
9 I. Cavaco, J. Costa Pessoa, M. T. L. Duarte, R. D. Gillard and P. M. Matias, *Chem. Commun.*, 1996, 1365.
10 S. Mondal, P. Ghosh and A. Chakravorty, *J. Chem. Soc.*, *Dalton Trans.*, 1997, 59.
11 A. Bernalte, F. J. G. Barros, I. Cavaco, J. Costa Pessoa, R. D. Gillard and F. J. Higes, *Polyhedron*, in the press.
12 J. A. Bonadies and C. J. Carrano, *J. Am. Chem. Soc.*, 1986, **108**, 4088.
13 N. D. Chasteen, in *Biological Magnetic Resonance*, eds. J. Lawrence, L. J. Berliner and J. Reuben, Plenum, New York, 1981, vol. 3, p. 53.
14 C. R. Cornman, E. P. Zovinka, Y. D. Boyajian, K. M. Geiser-Bush, P. D. Boyle and P. Singh, *Inorg. Chem.*, 1995, **34**, 4213.
15 EPRPOW, developed by L. K. White and R. L. Belford (University of Illinois) and modified by L. K. White, N. F. Albanese and N. D. Chasteen (University of New Hampshire) to include both Lorentzian and Gaussian line shape functions, an $I = 7/2$ nucleus, a 4th hyperfine interaction and multiple sites having different linewidths.
16 L. Casella, M. Gullotti, A. Pintar, S. Colona and A. Manfredi, *Inorg. Chim. Acta*, 1988, **144**, 89.
17 S. P. Rath, T. Ghosh and S. Mondal, *Polyhedron*, 1997, **16**, 4179.
18 G. Asgedom, A. Sreedhara, J. Kivikoski, J. Valkonen, E. Kolehmainen and C. H. Rao, *Inorg. Chem.*, 1996, **35**, 5674.
19 S. Liu and S. Gao, *Polyhedron*, 1998, **17**, 81.
20 A. A. Sagues, P. A. Williams and R. D. Gillard, *Transition Met. Chem.*, 1977, **2**, 55.
21 C. K. Johnson, ORTEP II, Report ORNL-5138, Oak Ridge National Laboratory, Oak Ridge, TN, 1976.
22 A. Durif, M. T. Averbuch-Pouchot and J. C. Guitel, *Acta Crystallogr.*, *Sect. B*, 1980, **36**, 680.
23 V. W. Day, W. G. Klemperer and D. J. Maltbie, *J. Am. Chem. Soc.*, 1987, **109**, 2991 and refs. therein.
24 D. H. Williams and I. Fleming, *Spectroscopic Methods in Organic Chemistry*, McGraw-Hill, London, 5th edn., 1995, p. 59.
25 A. García-Raso, J. J. Fiol, F. Bádenas and M. Quirós, *Polyhedron*, 1996, **15**, 4407.
26 J. J. R. Fraústo da Silva, R. Wootton and R. D. Gillard, *Chem. Commun.*, 1970, 3369.
27 J. Costa Pessoa, I. Cavaco, C. Madeira, M. T. Duarte, P. M. Matias and R. D. Gillard, 3rd GIPS Meeting in Inorganic Chemistry, SL 11, Senigallia, June 1995.
28 D. E. Metzler, M. Ikawa and E. E. Snell, *J. Am. Chem. Soc.*, 1954, **76**, 648.
29 H. Yamada and H. Kumagai, *Pure Appl. Chem.*, 1978, **50**, 1117.
30 E. W. Miles, in *Pyridoxal Phosphate and Derivatives*, eds. D. Dolphin, R. Poulson and O. Avramovic, Wiley, New York, 1986, p. 253.
31 F. Bergel, R. C. Bray and K. R. Harrap, *Nature* (*London*), 1958, **181**, 1654; F. Bergel, K. R. Harrap and A. M. Scott, *J. Chem. Soc.*, 1962, 1101.
32 A. Pasini and L. Casella, *J. Inorg. Nucl. Chem.*, 1974, **36**, 2133.
33 D. A. Phipps, *J. Mol. Catal.*, 1979, **5**, 81.
34 Yu. N. Belokon, N. G. Fallev, V. M. Belikov, V. A. Maksakov, P. V. Petrovskii and V. A. Tsyryapkin, *Bull. Acad. Sci. USSR*, *Div. Chem. Sci.*, 1977, 813.
35 R. L. Carlin, *Magnetochemistry*, Springer, Berlin, 1986, p. 11.
36 P. Lindroth and K. Mopper, *Anal. Chem.*, 1979, **51**, 1667.
37 R. Evens, J. Braven, L. Brown and I. Butler, *Chem. Ecology*, 1982, **1**, 99.
38 M. C. G. Alvarez-Coque, M. J. Hernández, R. M. V. Camanas and C. M. Fernández, *Anal. Biochem.*, 1989, **178**, 1.
39 G. M. Sheldrick, *Acta Crystallogr.*, *Sect. A*, 1990, **46**, 467.
40 G. M. Sheldrick and T. M. Schneider, *Methods Enzymol. B*, 1997, **277**, 319.

Paper 8/05768K